Theoretical calculations of heterojunction discontinuities in the Si/Ge system

Chris G. Van de Walle
Stanford Electronics Laboratories, Stanford University, Stanford, California 94305
and Xerox Corporation, Palo Alto Research Center, 3333 Coyote Hill Road,
Palo Alto, California 94304

Richard M. Martin
Xerox Corporation, Palo Alto Research Center, 3333 Coyote Hill Road, Palo Alto, California 94304
(Received 9 June 1986)

We present a theoretical study of the structural and electronic properties of pseudomorphic Si/Ge interfaces, in which the layers are strained such that the lattice spacing parallel to the interface is equal on both sides. The self-consistent calculations, based on the local density functional and *ab initio* pseudopotentials, determine the atomic structures and strains of minimum energy, and the lineup of the Si and Ge band structures. The presence of the strains causes significant shifts and splittings of the bulk bands. We derive values for the band discontinuities for (001), (111), and (110) interfaces under different strain conditions, and discuss the validity of the density-functional methods for the analysis of the interface problem. Spin-orbit splitting effects in the valence bands are included *a posteriori*. We express our results in terms of discontinuities in the valence bands, and deformation potentials for the bulk bands, and compare them with recent experiments on $Si/Si_{1-x}Ge_x$ heterostructures.

I. INTRODUCTION

It has recently become possible to grow epitaxial interfaces between materials which are lattice mismatched by several percent, using the technique of molecular-beam epitaxy (MBE). Lattice-mismatched heterostructures can be grown with essentially no misfit defect generation if the layers are sufficiently thin; the mismatch is then completely accommodated by uniform lattice strain.[1] The lattice constants parallel to the interfacial plane adjust so that perfect matching of the two materials is obtained. To compensate for this strain, the lattice constants perpendicular to the interface adjust independently for the two materials to minimize the elastic energy. This so-called pseudomorphic or commensurate growth[2] lowers the energy of the interfacial atoms, at the expense of stored strain energy within the coherently strained layers. These effects occur when a thin epitaxial layer is deposited on top of a substrate with a different lattice constant,[3] and also in strained-layer superlattices.[1] By growing layers on substrates of different lattice constants, or by modifying the ratio of the thicknesses of the layers in a free-standing superlattice, one can control the strains in the layers, and, as we shall see, modify significantly the electronic properties.

In this paper we will concentrate upon the Si/Ge heterojunction, for which the lattice constants of the pure elements Si and Ge are mismatched by 4%. Experimentally, dislocation-free interfaces have been grown between Si and $Si_{1-x}Ge_x$ alloys with a Ge fraction x of up to 75%, and even higher for very thin layers.[4] Si/Ge interfaces are interesting from a technological point of view because they offer the possibility of constructing heterojunctions which can be integrated directly with existing Si circuits.[5,6] Strained-layer structures also offer the advantage that band gaps can be shifted by the strains, giving added flexibility in the design of electronic components.[7] The large magnitudes of the strains may be illustrated by the example of a Si substrate with a thin layer of Ge on top. The Si substrate remains in the cubic structure, with a lattice constant $a_{Si}=5.43$ Å. The Ge layer (for which the unstrained lattice constant is $a_{Ge}=5.65$ Å) is compressed parallel to the interface, to match the Si lattice constant in the plane: $a_{\parallel}=5.43$ Å. It therefore needs to expand in the perpendicular direction, due to the Poisson effect. For a (100) interface, minimization of the elastic energy gives a perpendicular lattice constant for Ge: $a_{Ge\perp}=5.82$ Å. We will consider this case along with many others with greatly different strains.

We will mainly be interested in the heterojunction band lineups at the Si/Ge interfaces, information which is of crucial importance for all device applications. These band lineups will turn out to be dependent upon the interface orientation, and also upon the strain conditions in the materials. We will find, however, that results for intermediate strains can be found by interpolating between two extremes: one in which the Si is unstrained (cubic Si substrate with strained Ge), and the other in which Ge is unstrained (cubic Ge with strained Si). It therefore suffices to do the interface calculations for these extreme cases only. It also suffices to consider only interfaces between the pure materials Si and Ge; results for alloys can be obtained by interpolation.

Our calculations are performed on a superlattice geometry, as illustrated in Fig. 1. They are based on local-density-functional theory,[8] applied in the momentum space formalism,[9,10] and use nonlocal norm-conserving pseudopotentials.[11] These methods have been ap-

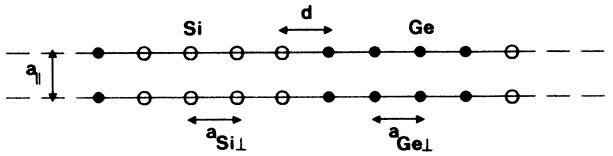

FIG. 1. Schematic illustration of a superlattice used for studying the Si/Ge interface. The supercell contains four atoms of each material and two interfaces. The lattice parameters $a_{||}$, $a_{Si\perp}$, $a_{Ge\perp}$, and d are defined.

plied to a wide variety of solid-state problems,[10,12,13] and provide a fundamental theoretical framework to address the problem. They allow us to calculate total energy, stress, and forces on the atoms, and thus determine the minimum energy structure of the interface. From the self-consistent potentials we obtain information about potential shifts at the interface. Combining this with bulk band-structure calculations will allow us to derive values for valence- and conduction-band discontinuities. Spin-orbit splitting effects in the valence bands are added in *a posteriori*. Finally, we need to consider the "band-gap problem,"[14] and examine to what extent the density-functional method is able to produce a reliable description of these heterojunction systems. Our discussion will indicate that for cases like Si/Ge the lineup of the bands should not be greatly modified by the known corrections to the local-density approximation.

Self-consistent calculations such as those performed in the present study provide the only way to take all the effects of the electronic structure of the interface into account. The present authors have used these methods to systematically study a wide variety of interface systems; specific results and some general conclusions have been reported elsewhere.[15–17] Other approaches to the heterojunction problem have included a number of "model" theories, such as those by Frensley and Kroemer,[18] Harrison,[19,20] Tersoff,[21,22] and by the present authors.[17] They all rely on certain assumptions to define a "reference level" for each semiconductor, which is then used in lining up the band structures. Although some of them are reasonably successful at predicting lineups, none can claim to take *all* the essential physics of the interface problem into account. The present *ab initio* calculations therefore provide a means of approaching the problem without making any uncontrolled assumptions. To our knowledge, they also constitute the first theoretical work to predict the band offsets at strained-layer interfaces.

In Sec. II, we will describe the strained-layer systems that we study, and show that these correspond to the minimum of total energy obtained from *ab initio* calculations. Section III will deal with how we extract information about band lineups from the self-consistent interface calculations, illustrated with the example of a (001) interface between cubic Si and strained Ge. We also examine some of the problems inherent to the local-density-functional approximation. In Sec. IV we will discuss how to express the splitting of the valence bands in terms of deformation potentials, incorporating spin-orbit splitting effects. Section V contains a further analysis of the strain effects on the band structure, and results for deformation potentials. In Sec. VI, we show full results for theoretical band lineups for various strains and interface orientations. Section VII will contain a comparison with other theories, and with some recent experimental findings on Si/Ge interfaces involving alloys of Si and Ge. The agreement will prove quite satisfactory. Some concluding remarks will be presented in Sec. VIII.

II. DETERMINATION OF THE STRUCTURE

The derivation of interface properties requires that one first determine the positions of the atoms of minimum energy, i.e., the structure of the interface. We do this by first constructing an ideal interface, following simple macroscopic rules, and then examining how close this *ansatz* is to the minimum energy structure as predicted by full self-consistent calculations. The strains in the materials, which are necessary to have a pseudomorphic interface, can be determined by minimizing the macroscopic elastic energy, under the constraint that the lattice constant in the plane, $a_{||}$, remains the same throughout the structure (lattice constants will be denoted by the letter a; the subscripts $||$ and $\perp$ are used to indicate lattice spacings parallel or perpendicular to the plane of the interface). For a system in which h_{Si} and h_{Ge} are the respective thicknesses of the (unstrained) Si and Ge layers, this yields the following results:

$$a_{||}=(a_{Si}G_{Si}h_{Si}+a_{Ge}G_{Ge}h_{Ge})/(G_{Si}h_{Si}+G_{Ge}h_{Ge}) , \quad (1)$$

$$a_{i\perp}=a_i[1-D^i(a_{||}/a_i-1)] , \quad (2)$$

where i denotes the materials, Si or Ge, a_i denotes the equilibrium lattice constants, and G_i is the shear modulus,

$$G_i=2(c^i_{11}+2c^i_{12})(1-D^i/2) . \quad (3)$$

The constant D depends on the elastic constants c_{11}, c_{12}, and c_{44} of the respective materials, and on the interface orientation:

$$D_{001}=2(c_{12}/c_{11}) , \quad (4a)$$

$$D_{110}=(c_{11}+3c_{12}-2c_{44})/(c_{11}+c_{12}+2c_{44}) , \quad (4b)$$

$$D_{111}=2(c_{11}+2c_{12}-2c_{44})/(c_{11}+2c_{12}+4c_{44}) . \quad (4c)$$

We should remark that for orientations other than the (001), the value given for $a_{||}$ does not correspond to the actual lattice constant in the crystallographic plane of the interface. Rather, $a_{||}$ and $a_{\perp}$ express how the dimensions of the appropriate unit cell change with respect to the unstrained bulk unit cell. The ratio of $a_{||}$ and $a_{i\perp}$ to the unstrained lattice constants determines the strain components parallel and perpendicular to the interface:

$$\epsilon_{i||}=(a_{||}/a_i-1) , \quad (5a)$$

$$\epsilon_{i\perp}=(a_{i\perp}/a_i-1) . \quad (5b)$$

We prefer using $a_{||}$ and $a_{\perp}$ instead of strain components, since this eliminates the need for defining a coordinate system and explicitly mentioning what material we are

TABLE I. Heterojunction band lineups for Si/Ge interfaces; $a_{||}$ and $a_{\perp}$ define the strain conditions of the materials, as described in the text; $\Delta E_v = E_{v,\mathrm{Ge}} - E_{v,\mathrm{Si}}$ is the discontinuity in the top of the valence band; $\Delta E_{v,\mathrm{av}} = E_{v,\mathrm{Ge,av}} - E_{v,\mathrm{Si,av}}$ is the discontinuity in the (weighted) average of the valence bands; $\Delta E_c = E_{c,\mathrm{Ge}} - E_{c,\mathrm{Si}}$ is the discontinuity in the minimum of the conduction band.

	$a_{\|\|}$ (Å)	$a_{\mathrm{Si}\perp}$ (Å)	$a_{\mathrm{Ge}\perp}$ (Å)	ΔE_v (eV)	$\Delta E_{v,\mathrm{av}}$ (eV)	ΔE_c (eV)
(001)	5.43	5.43	5.82	0.84	0.54	0.28
	5.52	5.36	5.75	0.61	0.53	0.41
	5.65	5.26	5.65	0.31	0.51	0.55
(111)	5.43	5.43	5.73	0.85	0.58	0.25
	5.65	5.33	5.65	0.37	0.56	0.28
(110)	5.43	5.43	5.75	0.76	0.52	0.03
	5.65	5.32	5.65	0.22	0.50	0.24

referring the strains to.

We notice from Eq. (1) that when $h_{\mathrm{Si}}/h_{\mathrm{Ge}} \to \infty$, then $a_{||} = a_{\mathrm{Si}}$; this corresponds to a Si substrate with strained Ge on top. Similarly, when $h_{\mathrm{Ge}}/h_{\mathrm{Si}} \to \infty$, then $a_{||} = a_{\mathrm{Ge}}$, corresponding to a Ge substrate. In general, if the layers are grown on a substrate, the value of $a_{||}$ is determined by the substrate and may be varied by using different substrates. However, for free-standing superlattices $a_{||}$ must be determined by equations such as (1). Once $a_{||}$ is known, $a_{i\perp}$ can be obtained using Eq. (2).

As an ansatz, we assume that the atoms occupy the ideal positions of the (appropriately strained) bulk lattice structure of each material up to the interface, and that the separation d between the Si and Ge layers at the interface is taken to be the average of the layer spacings in the two bulk materials. Now we examine to what extent these simple rules for deriving the atomic positions really yield the most stable structure, corresponding to the minimum energy configuration that can be found from the *ab initio* calculations. The most detailed study was performed for the case of the (001) interface between cubic Si at $a_{\mathrm{Si}} = 5.43$ Å and (001) strained Ge with $a_{||} = 5.43$ Å and $a_{\mathrm{Ge}\perp} = 5.82$ Å. We have carried out careful calculations of total energy and the forces on the atoms for a superlattice with four atoms per unit cell (two Si and two Ge). The results show that the minimum energy structure is very close to that we described above, within 0.1% for d and 1% for $a_{\mathrm{Ge}\perp}$. Furthermore, we will see in the next section that such small deviations from the ideal structure give rise to only very small changes in the heterojunction band lineups. We therefore conclude that determining the structure of the interface from macroscopic arguments is a very good ansatz. Incidentally, our result that d is equal to the average of the bulk values may be an example of a more generally applicable rule. Similar results were obtained for an Al/Ge interface by Batra.[23]

For the (111) and (110) pseudomorphic interfaces, the strains reduce the crystal symmetry in such a way that the separation of the two atoms in the bulk unit cell of the diamond structure is not uniquely determined from the macroscopic strain. When the materials are distorted along these directions, internal displacements of the atoms will occur. These are described by the internal displacement parameter ζ.[24] We used the values $\zeta_{\mathrm{Si}} = 0.53$ and $\zeta_{\mathrm{Ge}} = 0.44$, derived from theoretical calculations[10] which used exactly the same methods and potentials as we use here. In the case of strain along [111], the relative displacement of the two atoms in the unit cell is given by

$$\mathbf{u} = -(\zeta/6)(a_{\perp} - a_{||})(\hat{\mathbf{x}} + \hat{\mathbf{y}} + \hat{\mathbf{z}}) , \tag{6a}$$

where $\hat{\mathbf{x}}$, $\hat{\mathbf{y}}$, and $\hat{\mathbf{z}}$ are unit vectors along the Cartesian axes. For strain along [110], the expression is

$$\mathbf{u} = -(\zeta/4)(a_{\perp} - a_{||})\hat{\mathbf{z}} . \tag{6b}$$

No attempt was made to actually minimize the total energy for these structures. Based on our findings for the (001) interface, we assume that the actual positions of the atoms will be close to those found from macroscopic arguments.

From the description above, it follows that the strain situation of the system can be characterized fully by the interface orientation and the value of $a_{||}$, given the prescriptions for evaluating the strains by minimizing the elastic energy, and for calculating the internal displacements. In the following sections, we will describe the calculations that we have performed on (001), (111), and (110) interfaces. For each of these, we have examined the extreme cases in which all of the strain occurs in just one of the materials (i.e., $a_{||} = 5.43$ or 5.65 Å). For (001), we also examined an intermediate case ($a_{||} = 5.52$ Å), corresponding to a superlattice with layers of equal thickness; this allows us to draw conclusions concerning the linear behavior of the lineups as a function of strain. A list of the values of $a_{||}$, $a_{\mathrm{Si}\perp}$, and $a_{\mathrm{Ge}\perp}$ for the cases that we studied is given in Table I.

III. DERIVATION OF BAND LINEUPS

A. Self-consistent calculations

The fundamental problem in deriving the band lineups at heterojunctions is that for a bulk solid there is no intrinsic energy scale to which all energies are referred.[25] Therefore there can be no unique reference with which to compare the potentials for two different solids. The

reason for the ambiguity is that because of the long range of the Coulomb interaction, the zero of energy is undefined for an infinite (bulk) crystal. To derive the potential shift which occurs at the junction of two materials, one has to perform a calculation in which both types of materials are present. In the neighborhood of the interface, the electron distribution will clearly differ from the bulk, setting up a dipole moment which will cause shifts in the bands, even far from the interface. The only way to obtain a full picture of the interface problem is to carry out self-consistent calculations in which the electrons are allowed to adjust to the specific environment around the junction. Calculations have been done previously by Pickett *et al.*,[26] which followed this approach; however, they used empirical pseudopotentials, and considered only lattice-matched cases. In our studies, we have extended the method to strained-layer systems, and used the more recent *ab initio* pseudopotentials.[11] This term indicates that these potentials are generated using only theoretical calculations on atoms, without introducing any type of fitting to experimental band structures or other properties. This implies that, in contrast with the empirical approach, all elements are treated in the same way, which is particularly important when we want to include different materials in the same calculation, as for an interface.

Self-consistent solutions are obtained for the charge density and the total potential, which is the sum of ionic, Hartree, and exchange-correlation potentials. The latter is calculated using the Ceperley-Alder form.[27] In each cycle of iteration a potential is used for generating the charge density, from which a new potential can be calculated. This is then used for constructing the input for the next cycle. Convergence of the self-consistent iterations is obtained with the help of the Broyden scheme.[28] The first cycle requires a trial potential, for which we can choose the ionic potential screened by the dielectric function of a free-electron gas. An even better choice in many instances is the potential corresponding to a superposition of free-atom charge densities.

A major problem that has to be faced in calculating the electronic structure of an interface is the lack of translational invariance in the direction perpendicular to the interface. Our calculational approach assumes translational symmetry and exploits it in making Fourier expansions of the wave functions,[9,10] and in performing integrations over occupied states, using special points in the Brillouin zone.[29] We can artificially introduce periodicity into the problem by constructing a "supercell:" a large unit cell which consists of two slabs of the respective semiconductors in a particular orientation. This unit cell is then repeated and the electronic structure of the system is calculated self-consistently. A typical cell for the (001) orientation is shown in Fig. 1; it contains eight atoms and two identical interfaces. Of course, what we are really interested in are the results for an isolated interface. These can be derived from our calculations to the extent that the interfaces in the periodic structure are well separated. We will establish *a posteriori* that this is the case, by examining charge densities and potentials in the intermediate regions, and showing them to be bulklike.

We will describe in detail here the calculations performed for the (001) interface between cubic Si and strained Ge. Plane waves with kinetic energy up to 6 Ry were included in the expansion of the wave functions ($\approx$280 plane waves). A set of four special points was used for sampling k space.[29] Test calculations described later show that these choices are sufficient for the properties we are examining here. In the final self-consistent solution, a redistribution of electrons has occurred which changes the electric dipole in the interface region. The resulting self-consistent potential across the supercell is plotted in Fig. 2. Because the *ab initio* pseudopotentials used here are nonlocal, the total potential consists of different parts corresponding to different angular momenta l. We only show the $l=1$ part of the potential here. In the plot, the variation of the space coordinate $\mathbf{r}$ is limited to the component perpendicular to the interface, and values of the potentials are averaged over the remaining two coordinates, i.e., averaged in the plane parallel to the interface:

$$\bar{V}(z)=[1/(\mathrm{Na}^2)]\int V(\mathbf{r})dx\,dy\ . \tag{7}$$

In the regions far from the interface, the crystal should recover properties of the bulk. Therefore we also plot (dashed lines) the potentials determined separately from calculations on bulk Si and Ge (strained). We have chosen the average potential for the bulk crystals to agree with the interface calculation. One sees that already one layer away from the interface the potential assumes the form of the bulk potential. Similar results hold for the charge density. This confirms, *a posteriori*, that the two interfaces in our supercell are sufficiently far apart to be decoupled, at least as far as charge densities and potentials are concerned. The average levels of the ($l=1$) potentials which correspond to the bulk regions are also indicated in Fig. 2. We denote these average levels by $\bar{V}_{\mathrm{Si}}$ and $\bar{V}_{\mathrm{Ge}}$, and define the shift $\Delta\bar{V}=\bar{V}_{\mathrm{Ge}}-\bar{V}_{\mathrm{Si}}$.

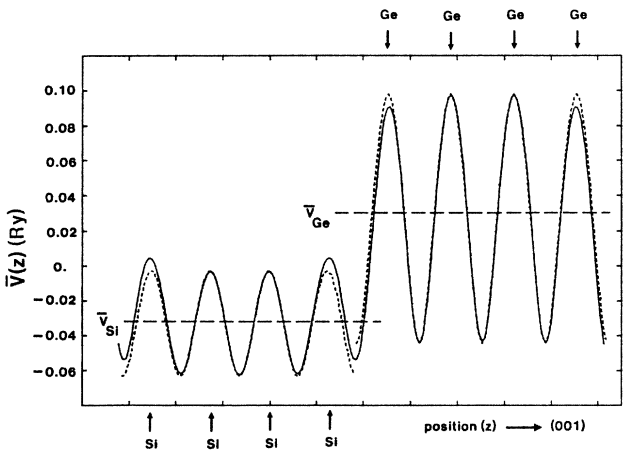

FIG. 2. Variation of the averaged $l=1$ component of the total potential $\bar{V}(z)$ [as defined in Eq. (7)] across the (001) interface. The dashed lines represent the corresponding potentials for the bulk materials. These coincide with $\bar{V}(z)$ in the regions far from the interfaces. However, the average levels of the two bulk potentials (dashed horizontal lines) are shifted with respect to each other.

To get information about band discontinuities, we still have to perform the band calculations for the bulk materials, i.e., cubic Si and Ge strained as in the superlattice layer. The energy cutoff has to be sufficiently high to make sure that energy *differences* are converged. It turns out that 12 Ry is sufficient for the valence bands; conduction bands, however, tend to show a larger dependence upon the cutoff, so calculations with cutoffs up to 18 Ry were performed to derive these values. We find that the valence-band maximum in Si is 11.19 eV above the average potential $\bar{V}_{\mathrm{Si}}$. In Ge, the strain along [001] splits the top of the valence band. The topmost valence band occurs at 11.08 eV, and the average energy of the three $\Gamma_{25'}$ valence band is 10.88 eV above $\bar{V}_{\mathrm{Ge}}$. Figure 3 illustrates the lineup procedure, using the result $\Delta\bar{V}=0.85$ eV, derived from Fig. 2. All values were consistently obtained with the $l=1$ component chosen as the reference potential; the band lineups, however, are independent of this choice. We see that this leads to a discontinuity in the highest valence band of $\Delta E_v=0.74$ eV (upward step in going from Si to Ge), or a discontinuity in the average valence-band energy of $\Delta E_{v,\mathrm{av}}=0.54$ eV. No spin-orbit splitting effects were taken into account in these calculations. In the next section, we will show how to incorporate these *a posteriori*. Our bulk band-structure calculations also give us conduction-band energies. In Si, the minimum of the conduction band occurs near the X point, at Δ. The conduction bands in Ge show significant shifts and splittings due to the strain; the lowest gap occurs at L, but the Δ minima are very close in energy. Following the same procedure as for the valence band, we find $\Delta E_c=0.28$ eV. We should point out that the magnitudes of the theoretical (local-density approximation) band gaps in each material do not agree with experiment; thus we leave the gaps undefined in the figure. ΔE_c, however, which is derived from the *relative* positions of the conduction bands, is *a priori* just as meaningful a quantity as is ΔE_v. We will discuss this in fuller detail below.

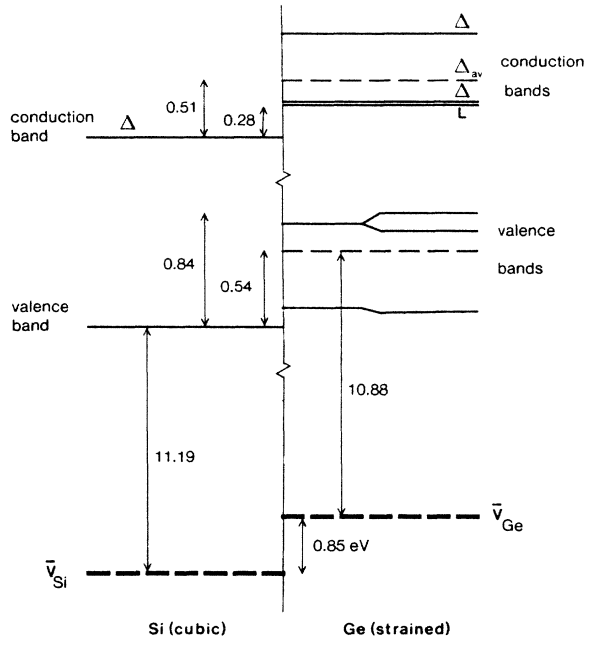

FIG. 3. Derivation of band lineups: relative position of the average potentials $\bar{V}_{\mathrm{Si}}$ and $\bar{V}_{\mathrm{Ge}}$, and of the Si and Ge valence and conduction bands. All values shown are derived with the $l=1$ angular momentum component chosen as the reference potential; the band lineups, however, are unique and independent of this choice. Band splittings result from strain in the materials; for Ge, the spin-orbit splitting is indicated separately. In each case, the weighted average of the bands is also given (dashed lines). The magnitude of the band gaps is left undefined in the figure; only the *relative* position of the conduction bands with respect to each other is meaningful. In Ge, both the conduction-band minima at Δ and at L are shown, as derived from the density-functional calculations without any adjustments.

We studied the sensitivity of our results to the procedures used. To test the dependence upon the energy cutoff, calculations were performed including more plane waves (up to 800), with kinetic energy up to 12 Ry. The effect on the shift in average potential was less than 0.04 eV. The direction of this shift is such that the valence-band discontinuity ΔE_v is slightly *lowered* at *higher* cutoffs. We have also examined the effects of using a larger number of special points in the integration over the Brillouin zone. At a constant energy cutoff of 6 Ry, we have increased the number of special points to eight or nine; the change in $\Delta\bar{V}$ was less than 0.01 eV. Next, an alternative verification of our assumption that the interfaces are sufficiently far apart was provided by performing a calculation on a cell with 12 atoms (six of each material). It was found that our result for the shift in averaged potentials is not significantly affected (by less than 0.02 eV) when we include more atoms, thus confirming that a cell with eight atoms suffices for our purposes. Finally, the effect of a rearrangement of the atoms near the interface was studied for the 12-atom cell. We displaced one plane of Ge atoms at the interface, corresponding to a 4% change in d, keeping all other atoms fixed. The resulting change in $\Delta\bar{V}$ was less than 0.02 eV. This indicates that our results for $\Delta\bar{V}$ (and ΔE_v) are not very sensitive to the details of the structure near the interface. Putting the information obtained from all the tests together, we expect the values for band lineups to be numerically precise to within 0.05—0.10 eV.

B. Comments on the accuracy of the local-density approximation

So far, we have used the results from self-consistent calculations on an interface supercell to derive the potential shift $\Delta\bar{V}$, and bulk band-structure calculations to derive the position of the valence and conduction bands with respect to the average potential $\bar{V}$. Density-functional theory was used throughout, and it is appropriate to consider what effects this method has upon the accuracy of the results. $\Delta\bar{V}$, as derived from the interface calculation, is associated with the dipole that is set up across the interface as a consequence of the redistribution of electrons. This quantity is really a ground-state property of the interface system, derived from information about filled

TABLE II. Comparison of the present theoretical results with experiment (Ref. 34 except where noted) for selected conduction-band critical points relative to the valence-band maximum in Si and Ge. The column labeled "Corr." gives the difference, i.e., the correction needed for the theory to agree with experiment.

	Si				Ge		
	Expt.	Theor.	Corr.		Expt.	Theor.	Corr.
Γ_{15}	3.37	2.55	0.82	$\Gamma_{2'}$	0.89	0.02	0.87
X_1	1.30	0.64	0.66	X_1	1.30	0.61	0.69
L_1	2.10[a]	1.45	0.65	L_1	0.74	0.09	0.65

[a]R. Hulthen and N. C. Nilsson, Solid State Commun. **18**, 1341 (1976).

valence states, and thus would be given exactly by the exact density-functional theory.[8] The successes of the local-density approximation for other ground-state properties lead to the expectation that it is reliably given by calculations such as the present work. Next, we consider the band energies with respect to $\bar{V}$, as derived from a bulk calculation. Here, we are confronted with the well-known problem that the band gaps of semiconductors are severely underestimated, even though the general topology of all bands is quite good. This deficiency of the density-functional method has been the focus of a number of theoretical investigations recently.[14] It is therefore appropriate to analyze this aspect of the computations in more detail.

In Table II, we give an overview of the calculated energies for a number of conduction-band critical points for unstrained Si and Ge, relative to the top of the valence band. The theoretical values were derived from bulk calculations with an energy cutoff of 18 Ry, using ten special points, and are essentially converged.[30] We also list experimental values, and the correction that needs to be applied to bring theory into agreement with experiment. Several conclusions can be drawn from this table. First, we notice that for each material the corrections at X and L are almost equal. The correction at Γ is slightly larger (by about 0.15 eV); this is to be expected, since the conduction bands at Γ are particularly sensitive to details of the pseudopotential, inclusion of relativistic effects, etc., as was pointed out by Bachelet *et al.*[31] However, this minimum of the conduction bands at Γ bears little relation to the conduction band as a whole, and has only a small volume of k space associated with it.[22] From a calculational point of view, none of the special points in our calculation is close to Γ, so the details of the band structure there will not influence the results. All this indicates that we can safely concentrate upon the indirect minima of the conduction band as the representative bands which will enter into the lineup procedure.[32] For these, we can draw the conclusion that the corrections in Si and Ge are very similar, differing by less than 0.1 eV. This has several important implications. First of all, it means that even though the theoretical band gaps of both materials are in disagreement with experiment, the corrections to the theoretical values are very similar on both sides, and thus the *relative* position of conduction bands is a meaningful quantity. We could have gone through the operation of shifting the conduction band in each material with respect to the valence band, to reproduce the experimental gap (the so-called "scissors operator"),[33] and afterwards looking at the conduction band lineups. Because these corrections are nearly equal on both sides, however, the *relative* position of the conduction bands would hardly be affected by this operation. Or, in other words, we can (to a good approximation) apply *one* scissors operator to shift the conduction bands on *both* sides of the heterojunction at once.

Apart from the practical advantages of this scheme, it has a more profound implication. So far, we have assumed that a bulk band-structure calculation gives us the positions of the bands with respect to the average potential $\bar{V}$. This is, of course, only true within the limitations of the local-density approximation, and certain corrections are necessary, for instance to bring the band gaps into agreement with experiment. One should keep in mind that such procedures may involve shifts not only of the conduction bands, but also of the valence band (with respect to $\bar{V}$).[14] However, as long as the corrections that need to be applied to the two materials are similar in magnitude (within the accuracy of the calculations), one can expect that this will not affect the ΔE_v and ΔE_c that we calculate (since the same scissors operator can be applied to both materials at once). Thus the corrections to the band *offsets* can be estimated to be on the order of the *difference* in the band-gap corrections that need to be applied to the two materials, which in the present case we saw to be approximately 0.1 eV. Therefore we conclude that our theoretical results for Si/Ge should describe the true band offsets to within ≈ 0.1 eV; for heterojunctions between more dissimilar materials, there may be larger corrections to the local-density results.

IV. STRAIN AND SPIN-ORBIT SPLITTING OF THE VALENCE BANDS

In the preceding section, we determined how to line up the band structures of two materials at the interface. We also pointed out that the presence of strains has a sizeable effect on the bulk bands. In this section, we will add the spin-orbit splitting. Since there is interaction between strain and spin-orbit splittings, we proceed by expressing the effects of strain upon the valence bands in terms of deformation potentials.

We have already shown that uniaxial strains give rise to

a splitting of the top of the valence band. So far, however, we have not talked about an additional effect on the valence bands at $\Gamma_{25'}$, namely the spin-orbit splitting. This effect was not taken into account in our density-functional calculations (although scalar relativistic effects were included by the use of the *ab initio* pseudopotentials[11]). For Si, the spin-orbit splitting of the valence band at Γ is quite small: $\Delta_0=0.04$ eV,[34] which is smaller than the accuracy of our calculations. We therefore neglect it altogether. For Ge, however, $\Delta_0=0.30$ eV,[34] which can give rise to more sizeable corrections. We assume that these corrections can be made *a posteriori*. For the unstrained material, this amounts to splitting the sixfold degenerate (including spin degeneracy) valence band at $\Gamma_{25'}$ into a higher-lying fourfold $p_{3/2}$ multiplet, and a lower-lying $p_{1/2}$ multiplet. These multiplets are separated by Δ_0, and their weighted average corresponds to the position of the sixfold degenerate band we found in our calculations. Practically, it means that in unstrained Ge the top of the valence band occurs at a position 0.1 eV higher in energy than found in our calculations. In the strained material, the spin-orbit and strain splittings will interact and produce a total splitting of the valence band, which can be conventionally expressed in terms of deformation potentials. From the equations in Ref. 35, the following shifts of the valence bands with respect to their weighted average are calculated for a uniaxial stress along [001]:

$$\Delta E_{v_2}=\tfrac{1}{3}\Delta_0-\tfrac{1}{2}\delta E_{001}\ , \tag{8a}$$

$$\Delta E_{v_1}=-\tfrac{1}{6}\Delta_0+\tfrac{1}{4}\delta E_{001}+\tfrac{1}{2}[\Delta_0^2+\Delta_0\delta E_{001}+\tfrac{9}{4}(\delta E_{001})^2]^{1/2}\ , \tag{8b}$$

$$\Delta E_{v_3}=-\tfrac{1}{6}\Delta_0+\tfrac{1}{4}\delta E_{001}-\tfrac{1}{2}[\Delta_0^2+\Delta_0\delta E_{001}+\tfrac{9}{4}(\delta E_{001})^2]^{1/2}\ . \tag{8c}$$

In these equations, Δ_0 is the experimental spin-orbit splitting at $\Gamma_{25'}$ in the unstrained material, and δE_{001} is the linear splitting of the multiplet. We have chosen the overall sign in Eqs. (8) such that a positive shift corresponds to raising the energy of the band. The band v_2 is a pure $|\frac{3}{2},\frac{3}{2}\rangle$ state, while v_1 and v_3 are mixtures of $|\frac{3}{2},\frac{1}{2}\rangle$ and $|\frac{1}{2},\frac{1}{2}\rangle$. δE_{001} can be expressed in terms of the magnitude of the strain and the deformation potential b, as follows:

$$\delta E_{001}=2b(\epsilon_{zz}-\epsilon_{xx})\ , \tag{9}$$

where $\epsilon_{xx}=(a_{||}-a_{\mathrm{Ge}})/a_{\mathrm{Ge}}$ and $\epsilon_{zz}=(a_{\perp,\mathrm{Ge}}-a_{\mathrm{Ge}})/a_{\mathrm{Ge}}$ are components of the strain tensor, and b is the appropriate deformation potential constant;[35] b is negative in Si and Ge.

The total splitting of the bands, in the absence of spin-orbit splitting, is equal to $\frac{3}{2}|\delta E_{001}|$; this is the value that we find from our density-functional calculations. Using the derived value of δE_{001}, and the experimental value of Δ_0, we can then obtain the positions of all multiplets by the use of Eqs. (8). From Eq. (9), we find that $\delta E_{001}<0$ for the case where Ge is strained to match a Si substrate. It can easily be checked from Eqs. (8) that the $v_2=|\frac{3}{2},\frac{3}{2}\rangle$ band will always be the one that is highest in energy, when $\delta E_{001}<0$. We therefore find that the only effect of taking spin-orbit splitting into account is to effectively shift the top of the valence band by 0.10 eV upward in energy, increasing the discontinuity ΔE_v by this value. The effect of incorporating the spin-orbit splitting in Ge is illustrated in Fig. 3. We should remark that the strains in the Ge layer are quite sizeable, such that strictly speaking we are outside the linear regime for which expressions such as Eqs. (8) and (9) were derived. Our procedure, however, starts from the explicitly calculated strain splittings, so no linearization is involved in deriving these. We therefore expect that use of Eqs. (8) to add the spin-orbit effects will give quite accurate results. If we want to use Eq. (9) to obtain a value for the deformation potential constant b, however, we should confine ourselves to the range of strains where nonlinearities are expected to be negligible. We have indeed performed calculations for bulk materials under smaller strains. For Si, we found $b=-2.35$ eV. This is very close to the value $b=-2.28$ eV obtained by Nielsen and Martin[10] from the same type of pseudopotential calculations as the present ones, but using a higher energy cutoff; it is also close to the value $b=-2.27$ eV obtained by Christensen,[36] using the linear muffin-tin orbital method. The experimental value[37] is $b=-2.10\pm0.10$ eV. For Ge, we found $b=-2.55$ eV (experiment[38] gives -2.86 ± 0.15 eV). These values are listed in Table III.

TABLE III. Theoretical and experimental values for selected deformation potentials of the $\Gamma_{25'}$ valence bands and Δ_1 and L conduction bands in Si and Ge, in eV.

	Si		Ge	
	Theor.	Expt.	Theor.	Expt.
$(\Xi_d+\frac{1}{3}\Xi_u-a)^\Delta$	1.72	1.50 ± 0.30[a]	1.31	
$(\Xi_d+\frac{1}{3}\Xi_u-a)^L$	−3.12		−2.78	$-2.0\ \pm0.5$[b]
b	−2.35	-2.10 ± 0.10[a]	−2.55	-2.86 ± 0.15[c]
d	−5.32	-4.85 ± 0.15[a]	−5.50	-5.28 ± 0.50[b]
Ξ_u^Δ	9.16	$8.6\ \pm0.4$[a]	9.42	
Ξ_u^L	16.14		15.13	$16.2\ \pm0.4$[b]

[a]Reference 37.
[b]Reference 40.
[c]Reference 38.

For the case of uniaxial stress along [111] [strained Ge on top of (111) Si], the equations are the same as for [001] above, with the quantity δE_{111} replacing δE_{001}. We see that, again, the topmost valence band in strained Ge will be shifted up by 0.10 eV due to inclusion of the spin-orbit splitting. For [111], the expression for the deformation potential is

$$\delta E_{111}=2\sqrt{3}d\epsilon_{xy} , \tag{10}$$

where $\epsilon_{xy}=\frac{1}{3}[(a_{\perp,\mathrm{Ge}}-a_{\mathrm{Ge}})/a_{\mathrm{Ge}}-(a_{\parallel}-a_{\mathrm{Ge}})/a_{\mathrm{Ge}}]$. In Si, we found $d=-5.32$ eV, to be compared with the other theoretical values, -5.47 eV (Ref. 10) and -5.29 eV (Ref. 36), and with experiment,[37] -4.85 ± 0.15 eV. In Ge, we found $d=-5.50$ eV (experiment,[38] -5.28 ± 0.50 eV).

In the case of uniaxial stress along [110], the situation is more complicated, as discussed in Ref. 35. No exact expressions can be written down for the energy levels; the splitting due to strain is a consequence of a mixture of the deformation potentials δE_{001} and δE_{111}. We therefore proceed as follows: we use the theoretical values of b and d, as derived above, together with the strain components ϵ_{xx}, ϵ_{zz}, and ϵ_{xy}, to calculate the value of the deformation potentials in this case. The expressions are

$$\delta E_{001}=4b(\epsilon_{xx}-\epsilon_{zz}) , \tag{11a}$$

$$\delta E_{111}=(4/\sqrt{3})d\epsilon_{xy} . \tag{11b}$$

We then use these values in the Hamiltonian matrix [Eq. (12) from Ref. 35] and calculate the eigenvalues. For the case without spin-orbit splitting, this reproduces the energy levels that we have derived independently from our density-functional calculations (to within 0.03 eV for the topmost band; the *shift* due to spin-orbit splitting will be predicted with even greater accuracy). Going through the numerical derivation, we find that putting in the spin-orbit splitting for strained Ge on top of Si leads to an upward shift of the top of the valence band by 0.09 eV. From now on, all values quoted for valence-band discontinuities will include the spin-orbit splitting in Ge.

V. DEFORMATION POTENTIALS IN Si AND Ge

In the preceding section, we analyzed the strain splitting of the valence bands in Si and Ge in terms of deformation potentials. A similar approach can be followed for the conduction bands; both the splitting of the bands as a result of the uniaxial strain, and the shift of the weighted average with respect to the valence band can be expressed in terms of deformation potentials. Following the notation of Herring and Vogt,[39,40] the energy shift of valley i for a homogeneous deformation described by the strain tensor $\overleftrightarrow{\epsilon}$ can be expressed as

$$\Delta E_c^i=[\Xi_d\overleftrightarrow{1}+\Xi_u\{\hat{\mathbf{a}}_i\hat{\mathbf{a}}_i\}]:\overleftrightarrow{\epsilon} \tag{12}$$

where $\overleftrightarrow{1}$ is the unit tensor, $\hat{\mathbf{a}}_i$ is a unit vector parallel to the $\mathbf{k}$ vector of valley i, and $\{\ \}$ denotes a dyadic product. The shift of the mean energy of the conduction-band extrema is

$$\Delta E_c^0=(\Xi_d+\tfrac{1}{3}\Xi_u)\overleftrightarrow{1}:\overleftrightarrow{\epsilon}. \tag{13}$$

The quantity $(\Xi_d+\frac{1}{3}\Xi_u)$ is sometimes denoted as E_1.[41] The shift in the mean energy of the valence-band extrema (at $\mathbf{k}=\mathbf{0}$) is given by

$$\Delta E_v^0=a\overleftrightarrow{1}:\overleftrightarrow{\epsilon}. \tag{14}$$

From Eqs. (13) and (14), the shift in the mean energy gap is

$$\Delta E_g^0=(\Xi_d+\tfrac{1}{3}\Xi_u-a)\overleftrightarrow{1}:\overleftrightarrow{\epsilon}. \tag{15}$$

The quantities $(\Xi_d+\frac{1}{3}\Xi_u)$ and a are difficult to calculate or measure, since they refer to changes in the bands on an *absolute* scale;[42,43] $(\Xi_d+\frac{1}{3}\Xi_u-a)$, however, refers to *relative* changes in the band positions (of conduction band with respect to valence band), and can straightforwardly by extracted from our calculations. Results for this deformation potential are given in Table III for Si and Ge, and are compared with experimental values. Experiments typically concentrate on the lowest gap (Δ in Si, L in Ge); we were not able to find any experimental values for Δ in Ge, or L in Si.

Next, we consider the splittings of the bands with respect to the mean energy. For the valence bands, we have already discussed this in Sec. IV, and have given results for the deformation potentials b and d. These are also listed in Table III. For the conduction bands, we first consider the minima of the conduction band at Δ, near the X-points. Uniaxial strain along [111] leaves these minima degenerate. Under uniaxial strain along [001] or [110], however, they become inequivalent: The bands along [100] and [010] will split off from the one along [001]. The splitting of the bands with respect to the mean energy is then given by

$$+\tfrac{2}{3}\Xi_u^{\Delta}(\epsilon_{zz}-\epsilon_{xx})$$

for the bands along [001]and $[00\bar{1}]$,and (16)

$$-\tfrac{1}{3}\Xi_u^{\Delta}(\epsilon_{zz}-\epsilon_{xx})$$

for the bands along [100], $[\bar{1}00]$, [010], and $[0\bar{1}0]$. The superscript Δ on Ξ_u indicates which conduction-band valley we are considering. Sometimes the notation E_2 is used instead of Ξ_u.[41]

Next, let us consider the conduction bands at L. They remain degenerate under [001] strain, but split under [111] strain according to

$$+2\Xi_u^L\epsilon_{xy}$$

for the band along [111], and (17)

$$-\tfrac{2}{3}\Xi_u^L\epsilon_{xy}$$

for the bands along $[\bar{1}11]$, $[1\bar{1}1]$, and $[11\bar{1}]$. Under [110] strain, the splitting becomes

$$+\tfrac{2}{3}\Xi_u^L\epsilon_{xy}$$

for the bands along [111] and $[11\bar{1}]$,and (18)

$$-\tfrac{2}{3}\Xi_u^L\epsilon_{xy}$$

for the bands along $[\bar{1}11]$ and $[1\bar{1}1]$. Results for Ξ_u^{Δ} and Ξ_u^L are given in Table III for Si and Ge. Once again, we

could only find experimental information on the Δ gap in Si, and the L gap in Ge. We should remark that the deformation potentials d and Ξ_u^L are quite sensitive to the value of the internal displacement parameter ζ. We have assumed here that the value of ζ, obtained by careful calculations in Ref. 10, is the most appropriate one to use.

We now have calculated all the information we need to derive band discontinuities: $\Delta\bar{V}$ (or $\Delta E_{v,\mathrm{av}}$) tells us how to line up the band structures, and the deformation potentials describe the changes in the bulk bands due to the strain. In the rest of the paper we will show results, and apply them to practical situations.

VI. RESULTS FOR BAND DISCONTINUITIES

Table I contains a summary of our results for all the interface orientations we have studied, for different strain conditions (as specified by $a_{||}$, $a_{\mathrm{Si}\perp}$, and $a_{\mathrm{Ge}\perp}$). The values of ΔE_v include the spin-orbit splittings, as discussed in Sec. IV. This accounts for the difference with previously published values,[15] which did not take spin-orbit splittings into account. We consider the (001) orientation in most detail, since that is the one used in the experimental studies on pseudomorphic interfaces that have been reported so far.[44,45] ΔE_v refers to the discontinuity in the *top* of the valence bands at $\Gamma_{25'}$. For the (001) interface, we see that it varies almost linearly with $a_{||}$; this justifies linear interpolation between the two extreme cases ($a_{||}=5.43$ and 5.65 Å) to obtain ΔE_v for intermediate values of $a_{||}$:

$$\Delta E_v(a_{||})=0.84-2.41(a_{||}-5.43)\ , \tag{19}$$

where $a_{||}$ is in Å, and ΔE_v is in eV.

$\Delta E_{v,\mathrm{av}}$ refers to the discontinuity in the weighted average of the valence bands at $\Gamma_{25'}$; by performing such an average, we eliminate the splittings due to strain and spin-orbit effects (while keeping the shifts due to volume changes). For all orientations, we notice that $\Delta E_{v,\mathrm{av}}$ is almost constant: $\Delta E_{v,\mathrm{av}}=0.54\pm0.04$ eV. This suggests that $\Delta E_{v,\mathrm{av}}$ might qualify as a parameter characteristic of the heterojunction, irrespective of the orientation and strain conditions. The splittings of the bands under strain are such, though, that the discontinuities as measured from the top of the valence bands vary by quite a large amount. This is clearly illustrated in Fig. 4, which shows valence- and conduction-band lineups for two extreme cases in the (001) orientation: Figure 4(a) for a heterojunction between cubic Si and strained Ge ($a_{||}=5.43$ Å), and Fig. 4(b) for a heterojunction between cubic Ge and strained Si ($a_{||}=5.65$ Å). We do not make any attempt to obtain the correct value of the band gaps; as explained above, an overall shift of the conduction bands on both sides of the interface could take care of that to within ≈0.1 eV. In the figure, we leave the value of the gaps undefined.

Table I also contains values for ΔE_c. For Si, the lowest conduction band always occurs at Δ, close to the X point. The shift in the conduction band is due to a change in the average band gap, caused by the hydrostatic part of the strain, and a splitting of the band due to the uniaxial components of the strain. We mentioned in Sec. V that strain along [001] or [110] splits the bands at Δ (the bands along

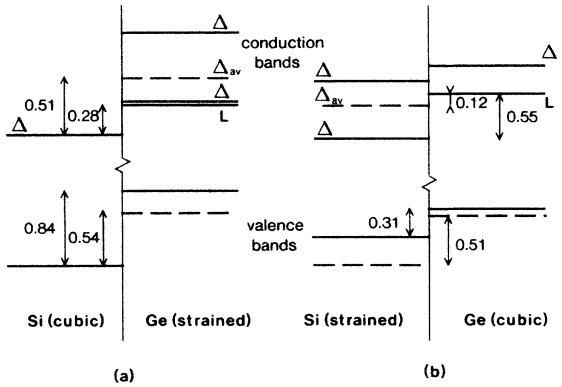

FIG. 4. Band-structure discontinuities: Relative position of the Si and Ge valence and conduction bands. Band splittings result from strain and spin-orbit splittings in the materials; in each case, the weighted average (dashed line) is also given. (a) is for the case $a_{||}=5.43$ Å (cubic Si, strained Ge). (b) is for $a_{||}=5.65$ Å (cubic Ge, strained Si). The magnitude of the band gaps is left undefined in the figure; only the *relative* position of the conduction bands with respect to each other is meaningful. Both the conduction-band minima at Δ and at L are given for Ge.

[100] and [010] become inequivalent to the one along [001]), while strain along [111] leaves the Δ minima degenerate. For Ge, the situation is somewhat more complicated. In the unstrained material, the minimum of the conduction band occurs at the L point. The bands at this point are split by a [111] or a [110] uniaxial strain. In the next section, we will compare our results with experiments on interfaces between Si and $\mathrm{Si}_{1-x}\mathrm{Ge}_x$ alloys. In alloys with Ge composition below 85%, the minimum of the conduction band occurs at Δ, as in Si.[46] Since we shall obtain results for alloys by interpolation between Si and Ge, it is important to also study this conduction-band minimum Δ. It turns out that the theoretical results for ΔE_c at the pure Si/Ge interfaces, as given in Table I, all involve the minimum at L in Ge as the lowest conduction-band point. The relative positions of the different conduction-band minima for two extreme cases of a (001) interface are illustrated in Fig. 4.

VII. COMPARISON WITH OTHER THEORIES AND WITH EXPERIMENT

Finally, we would like to compare our results on interfaces with other theoretical and experimental information that is available. As we emphasized throughout this paper, the values of band discontinuities for a pseudomorphic interface like Si/Ge are very sensitive to the particular strain situation of the layers. Unfortunately, most of the experimental values for ΔE_v that have been reported[47–49] did not specify the exact structure of the interface. Kuech *et al.*[47] used a chemical vapor deposition technique to deposit Ge on (001) Si, and estimated the band discontinuities from reverse-bias capacitance measurements. They found $\Delta E_v=0.39\pm0.04$ eV and $\Delta E_c=0.05\pm0.04$ eV. Margaritondo *et al.*[48] used photoemission spectro-

scopy to determine shifts in core levels and valence-band edges for thin overlayers of Ge on (111) Si, leading to $\Delta E_v = 0.2$ eV; they noted that different sample-preparation techniques do not change ΔE_v by more then 0.2 eV. Mahowald *et al.*,[49] using the same technique, obtained $\Delta E_v = 0.4 \pm 0.1$ eV for thin overlayers of Si on (111) Ge. Presumably the interfaces that were studied in all these cases were not pseudomorphic, and may have contained a large number of dislocations to relieve the strain. It is not clear what value of ΔE_v to expect in such a case. It is tempting to consider $\Delta E_{v,\mathrm{av}}$, which turns out to be nearly the same for all orientations and strain situations that we looked at—but one should not forget that $\Delta E_{v,\mathrm{av}}$, while eliminating the splitting effects due to the uniaxial components of the strain, still contains a contribution due to the volume change (hydrostatic component of the strain). This contribution would also be absent for interfaces which are not pseudomorphic, so that even $\Delta E_{v,\mathrm{av}}$ cannot be simply related to any of the measured values for nonpseudomorphic heterostructures.

The same type of problem occurs when we try to compare our values with the results from model theories like Harrison's [predicting $\Delta E_v = 0.38$ eV (Ref. 19) or 0.29 eV (Ref. 20)], or Tersoff's[21] (which predicts $\Delta E_v = 0.18$ eV). These theories are based upon the derivation of a reference level for each bulk semiconductor. These levels are then matched up at the interface, and determine the band lineups. It should, in principle, be possible to include the effects of strain within these models; however, no prescription to that extent was given by their authors, so that it is not clear what the resulting lineups are for a pseudomorphic interface.

Recently, however, several experimental groups have succeeded in growing dislocation-free pseudomorphic $Si/Si_{1-x}Ge_x$ interfaces, and performing measurements which, while not yielding an explicit value for ΔE_v, still provide qualitative information about the band lineups. It is interesting to check whether our theoretical band lineups agree with the experimental results. To do this, we will construct plots which will contain all the necessary information to determine the valence- and conduction-band lineups for a number of experimentally interesting interfaces between Si or Ge and $Si_{1-x}Ge_x$ alloys. So far, we have only shown results for interfaces between pure Si and Ge. To derive results for alloys, we propose to interpolate the results for ΔE_v. Although this is not *a priori* obvious, it is supported by our finding that the average $\Delta E_{v,\mathrm{av}}$ was almost constant for all strains tested; furthermore, we have found ΔE_v to be additive and transitive for a great number of different interfaces,[16] and to be well described by a simple model that is manifestly linear in the alloying.[17] This is not true for the conduction bands, and we should not attempt to interpolate ΔE_c. Since nonlinearities in the band gap are known,[46] we thus assume that they occur in the relative positions of the conduction bands. We therefore use experimental information about band gaps, in conjunction with ΔE_v, to derive ΔE_c.

To approach the problem systematically, we will consider the hydrostatic and uniaxial components of the strain separately when examining their influence on the bulk band structure. The uniaxial components introduce a splitting with respect to the (weighted) average of valence and conduction bands. The relative position of the average valence and conduction band is affected by the hydrostatic component. To determine how to line up the band structures on either side of the interface, we will focus upon the *average* valence-band discontinuity $\Delta E_{v,\mathrm{av}}$ for the reasons mentioned above. Figure 5 shows $\Delta E_{v,\mathrm{av}}$ for $Si_{1-x}Ge_x$ alloys, grown on Si(001) substrates: it changes linearly between 0 eV (pure Si on Si) and 0.53 eV [average of the $\Delta E_{v,\mathrm{av}}$ values for pure Ge on Si(001), from Table I]. The uniaxial component of the strain in the alloy leads to a splitting of the valence band. This splitting, including spin-orbit effects, was calculated in Sec. IV [Eqs. (8)]. For the alloy, we perform a linear interpolation for the values of δE_{001} (strain splitting) and Δ_0 (spin-orbit splitting), between 0 and the value for pure Ge. Due to the nature of Eqs. (8), this leads to a slight (almost unnoticeable) nonlinearity in the splitting of the valence band for the alloy.

To put the conduction bands into the picture, we use the experimental alloy band-gap data from Ref. 46. This determines where to place the (average) conduction band with respect to the (average) valence band in the alloy, provided we include the shift in the band gap due to the hydrostatic component of the strain. This shift is, once again, found by linear interpolation starting from our calculated value for pure Ge. In a next step, we introduce the splitting of the conduction band. It is important to point out that the lowest conduction band in the un-

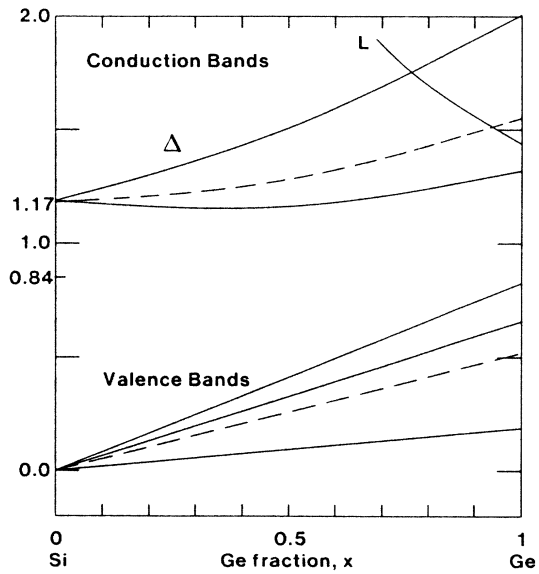

FIG. 5. Valence and conduction bands in strained $Si_{1-x}Ge_x$ alloys, matched to a Si(001) substrate. All energies are referred to the top of the valence band in Si. The weighted averages of the valence bands and of the Δ conduction bands are indicated with dashed lines. Values for valence-band discontinuities, hydrostatic shifts of the gaps, and strain splittings of the bands were derived from self-consistent calculations on pure Ge, and interpolated to derive results for alloys. Band gaps for the unstrained material were taken from experiment (Ref. 46).

strained alloy has Δ character up to 85% Ge, and becomes L-like above that. Therefore, we include both minima in the plot. For alloys on Si(001) substrates, the conduction band at L shows no splitting, and the minimum at Δ is lower over the whole range of alloy compositions.

The distance between the top of the valence band and the lowest conduction band tells us what the band gap is in the alloy with Ge fraction x, appropriately strained to match a Si(001) substrate. In Fig. 6 we plot the distance from the v_1 and v_2 valence bands to the lowest conduction band, and compare it with experimental data from Ref. 45. We see that the agreement is better than 0.05 eV; the small deviations may be due to inaccuracies in the (unstrained) alloy band gap.[46] We see that the alloy gap is significantly narrowed by the strain, in comparison with the unstrained material.

Let us now compare the results of Fig. 5 with experimental information. People *et al.*[50] have observed modulation doping effects in $Si/Si_{0.8}Ge_{0.2}$ heterojunctions grown by molecular-beam epitaxy. High peak hole mobilities at low temperatures were measured, indicating the presence of a two-dimensional hole gas at the heterointerface. Since the occurrence of modulation doping requires a sufficiently large discontinuity in the band edge, these results shed light on the relative band alignment between Si and $Si_{0.8}Ge_{0.2}$. Identical measurements on n-type heterojunctions failed to show a sustained enhancement of the mobility at low temperatures. This was interpreted as evidence that $\Delta E_v \gg \Delta E_c$. From Fig. 5 we find that for $x=0.2$, $\Delta E_v = 0.17$ eV, which is sufficient to observe modulation doping effects for holes. In contrast, Fig. 5 shows that ΔE_c is essentially zero. Therefore, no n-type modulation doping effect is expected to be observed, in agreement with the experimental results.[50] This result for ΔE_c is very close to that obtained by People and Bean,[7] who used our values for ΔE_v (without spin-orbit splitting, however), in conjunction with experimental deformation potentials to derive ΔE_c.

We have constructed a number of other plots, which may be useful in studying practical applications of the strained-layer interfaces. Figure 7 shows results for an alloy layer deposited on a Ge substrate. Here, we notice that in the range $0.8 < x < 1.0$ the alloy band gap is larger than the Ge gap, which leads to a type-I (straddling) lineup, with the Ge gap completely inside the alloy gap. Figures 8 and 9, finally, give information about the lineups for (111) and (110) interfaces. When strained in the [111] direction, the alloy does not show any splitting of the Δ minimum, in contrast to the minimum at L. For strains in the [110] direction, both conduction-band minima are split. We should remark that the ΔE_c values for pure Si/Ge interfaces that can be derived from Figs. 5, 7, 8, and 9 (i.e. at the end points $x=0$ or $x=1$) may be slightly different from those listed in Table I. That is because the values in the table are directly derived from the calculations, whereas the ones in the figures have been adjusted to reproduce the experimental band gaps. In particular, the Δ gap in Ge, as extrapolated from the alloy data of Ref. 46, occurs at a lower energy with respect to other conduction-band features than in the calculations. This brings it below the L gap for pure Ge on top of (001) Si (Fig. 5) or (110) Si (Fig. 9).

Now we would like to compare our results with the ex-

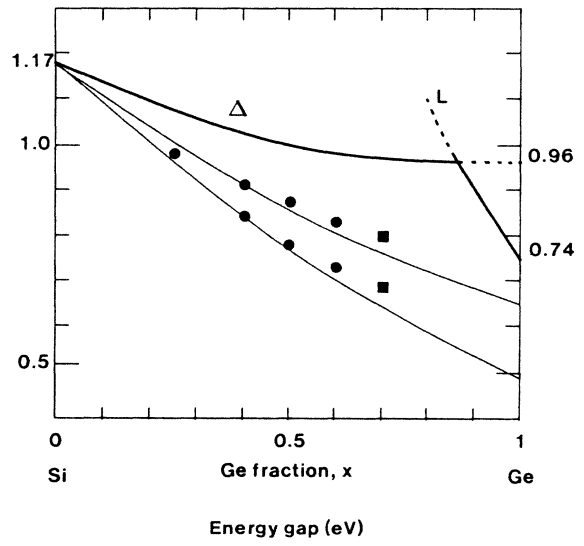

FIG. 6. Energy gap of strained $Si_{1-x}Ge_x$ alloys, matched to a Si substrate. The top curve shows the experimental data for the unstrained alloy band gap (from Ref. 46). Values for hydrostatic shifts of the gaps and strain splittings of the bands were derived from self-consistent calculations on pure Ge, and interpolated to derive results for alloys. We plot the distance between the v_1 and v_2 valence bands, and the lowest conduction band. Circles and squares correspond to experimental data from Ref. 45.

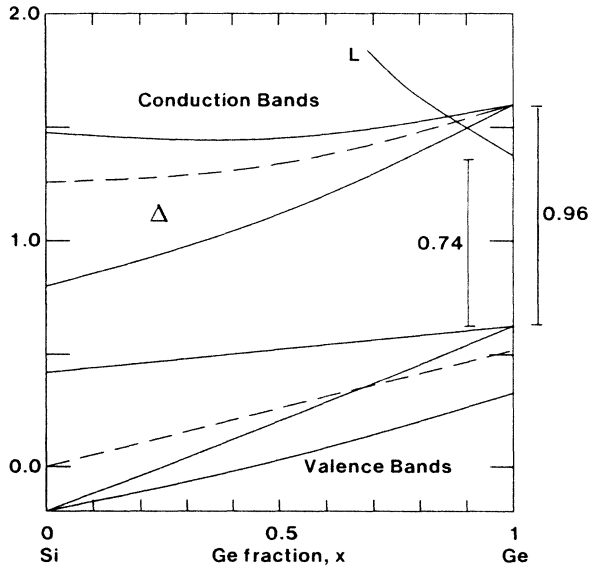

FIG. 7. Valence and conduction bands in strained $Si_{1-x}Ge_x$ alloys, matched to a Ge(001) substrate. All values were derived and plotted in the same way as in Fig. 5.

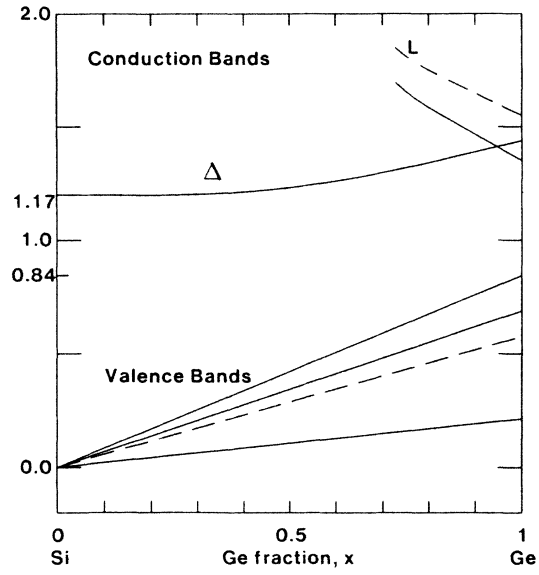

FIG. 8. Valence and conduction bands in strained $Si_{1-x}Ge_x$ alloys, matched to a Si(111) substrate. All values were derived and plotted in the same way as in Fig. 5.

periments of Abstreiter *et al.*[44] They have done experiments on a (001) superlattice consisting of a periodic sequence of equally thick Si and $Si_{0.5}Ge_{0.5}$ layers. This structure was grown on a buffer layer of $Si_{0.75}Ge_{0.25}$ in order to achieve a medium lattice spacing between that of Si ($a_{Si}=5.43$ Å) and that of $Si_{0.5}Ge_{0.5}$ ($a_{alloy}=5.54$ Å). Enhanced electron mobilities were found in samples where the $Si_{0.5}Ge_{0.5}$ layers were doped. This indicates that, even

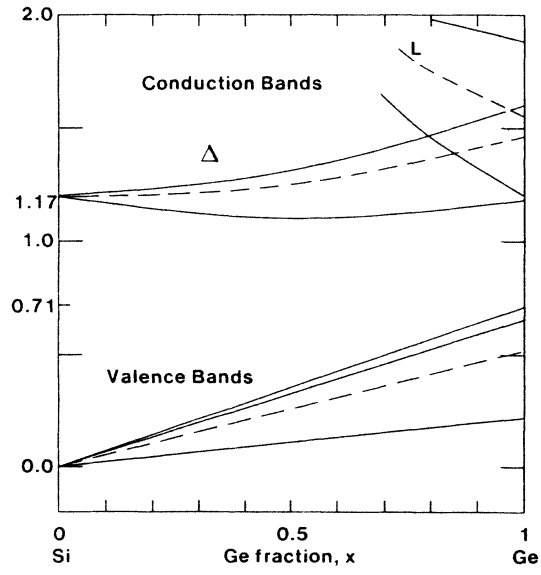

FIG. 9. Valence and conduction bands in strained Si_{1-x} Ge_x alloys, matched to a Si(110) substrate. All values were derived and plotted in the same way as in Fig. 5.

though this is the smaller band-gap material, the conduction-band edge in $Si_{0.5}Ge_{0.5}$ would be higher than in Si. We will use this structure as an example to illustrate how to derive the lineups in a general case. Both types of layers are strained here; applying Eqs. (1)–(4), with elastic constants for the alloy obtained by interpolation, we find that $a_{||}=5.48$ Å, $a_{Si\perp}=5.39$ Å, and $a_{alloy\perp}=5.59$ Å. Proceeding as described above, we obtain $\Delta E_{v,av}=0.265$ eV. From the values of $a_{||}$ and $a_{Si\perp}$, we find $\epsilon_{xx}=\epsilon_{yy}=9.21\times10^{-3}$, and $\epsilon_{zz}=7.37\times10^{-3}$ in Si. We now calculate the positions of valence and conduction bands. Equation (9) gives $\delta E_{001}=0.078$ eV; the top of the valence band will be raised by this amount above the weighted average. From Eq. (15), we find that $\Delta E_g^0=0.019$ eV. Finally, the lowest conduction band will be 0.101 eV below the mean [Eq. (16)]. The gap in Si is therefore equal to $(1.17+0.019-0.078-0.101)$ eV$=1.01$ eV. For the alloy, we calculate the change in band gap by interpolating the values of the deformation potentials. We find from Table III: $b=-2.45$ eV, $(\Xi_d+\frac{1}{3}\Xi_u-a)^{\Delta}=1.515$ eV, and $\Xi_u^{\Delta}=9.29$ eV. This leads to $\delta E_{001}=-0.094$ eV, a shift for the top of the valence band of 0.097 eV, $\Delta E_g^0=-0.020$ eV, and a lowering of the conduction band by 0.059 eV. The unstrained alloy band gap at $x=0.5$ is 0.99 eV (Fig. 6); since we are referring all energies to the *mean* valence band, we have to add 0.05 eV to this to compensate for spin-orbit splitting. The strained alloy band gap is therefore equal to $(0.99+0.05-0.020-0.097-0.059)$ eV$=0.86$ eV. Finally, we obtain $\Delta E_v=(0.265+0.0097-0.078)$ eV$=0.28$ eV, and $\Delta E_c=\Delta E_v+E_g^{alloy}-E_g^{Si}=0.13$ eV. The conclusion is that we find the conduction band on the $Si_{0.5}Ge_{0.5}$ side to be above the conduction band on the Si side, which agrees with Abstreiter's results (type-II lineup). Note that this result is quite different from what one would have obtained for $Si_{0.5}Ge_{0.5}$ layers on an unstrained Si substrate. The band lineups in that case can be derived from Fig. 5: $\Delta E_v=0.38$ eV, $E_g^{alloy}=0.77$ eV, and therefore $\Delta E_c=(0.38+0.77-1.17)$ eV$=-0.02$ eV, which corresponds to a type-I lineup.

VIII. CONCLUSIONS

In this paper, we have presented the first fully self-consistent theoretical study of atomic and electronic structure of pseudomorphic Si/Ge interfaces. Our total-energy calculations have led to the conclusion that the structure of the interface can be determined from macroscopic arguments, with the strains determined by the minimum of the elastic energy, and the interplanar distance at the interface by the average of the bulk distances. The results for band discontinuities depend strongly upon the specific strain conditions. The valence-band discontinuity, ΔE_v, can be changed by as much as 0.5 eV by varying the strain, and the lineups can be changed from type I to type II. It is convenient to express them in terms of the discontinuity in the average of the valence bands, $\Delta E_{v,av}$ (Table I), which determines how to line up the band structures of the appropriately strained bulk materi-

als. The shifts and splittings of the bulk bands can be expressed in terms of deformation potentials, for which we have given results in Table III. This approach makes it possible to obtain results for alloys by linear interpolation; the comparison with experiments on pseudomorphic interfaces[44,45,50] is satisfactory. Together with theoretical arguments about the validity of the local-density approximation, this gives us confidence that the self-consistent density-functional method provides a valuable fundamental approach to the interface problem.

ACKNOWLEDGMENTS

We are indebted to K. Kunc, O. H. Nielsen, and R. J. Needs, whose developments we have used. Conversations with G. Abstreiter, J. C. Bean, M. Cardona, W. C. Herring, J. Northrup, R. People, F. H. Pollak, J. Tersoff, W. A. Harrison, and W. E. Spicer are gratefully acknowledged. This work was partially supported by U.S. Office of Naval Research (ONR) Contract No. N00014-82-C0244.

[1]G. C. Osbourn, J. Appl. Phys. **53**, 1586 (1982).

[2]J. H. Van der Merwe and N. G. Van der Berg, Surf. Sci. **32**, 1 (1972).

[3]J. H. Van der Merwe, J. Appl. Phys. **34**, 123 (1963); J. H. Van der Merwe and C. A. B. Ball, in *Epitaxial Growth,* edited by J. Matthews (Academic, New York, 1975), Part b.

[4]R. People, J. C. Bean, D. V. Lang, A. M. Sergent, H. L. Störmer, K. W. Wecht, R. T. Lynch, and K. Baldwin, Appl. Phys. Lett. **45**, 1231 (1984); J. C. Bean, L. C. Feldman, A. T. Fiory, S. Nakahara, and I. K. Robinson, J. Vac. Sci. Technol. A **2**, 436 (1984); J. C. Bean, in *Proceedings of the First International Symposium on Silicon Molecular Beam Epitaxy,* edited by J. C. Bean (Electrochemical Society, Pennington, N.J., 1985), pp. 339–350.

[5]E. Kasper, H. J. Herzog, and H. Kibbel, Appl. Phys. **8**, 199 (1975).

[6]J. C. Bean, Science **230**, 127 (1985).

[7]R. People and J. C. Bean, Appl. Phys. Lett. **48**, 538 (1986).

[8]P. Hohenberg and W. Kohn, Phys. Rev. **136**, B864 (1964); W. Kohn and L. J. Sham, *ibid.* **140**, A1133 (1965).

[9]J. Ihm, A. Zunger, and M. L. Cohen, J. Phys. C **12**, 4409 (1979).

[10]O. H. Nielsen and R. M. Martin, Phys. Rev. B **32**, 3792 (1985).

[11]G. B. Bachelet, D. R. Hamann, and M. Schlüter, Phys. Rev. B **26**, 4199 (1982).

[12]R. M. Martin, in *Festkörperprobleme (Advances in Solid State Physics),* edited by P. Grosse (Vieweg, Braunschweig, 1985), Vol. XXV, pp. 3–17.

[13]K. Kunc and R. M. Martin, Phys. Rev. B **24**, 3445 (1981).

[14]C. S. Wang and W. E. Pickett, Phys. Rev. Lett. **51**, 597 (1983); L. J. Sham and M. Schlüter, *ibid.* **51**, 1888 (1983); M. S. Hybertsen and S. G. Louie, Phys. Rev. B **30**, 5777 (1984); Phys. Rev. Lett. **55**, 1418 (1985).

[15]C. G. Van de Walle and R. M. Martin, J. Vac. Sci. Technol. B **3**, 1256 (1985).

[16]C. G. Van de Walle and R. M. Martin, in *Computer-Based Microscopic Description of the Structure and Properties of Materials* (Materials Research Society, Pittsburgh, 1986), Vol. 63.

[17]C. G. Van de Walle and R. M. Martin, J. Vac. Sci. Technol. B **4**, 1055 (1986).

[18]W. R. Frensley and H. Kroemer, J. Vac. Sci. Technol. **13**, 810 (1976).

[19]W. A. Harrison, *Electronic Structure and the Properties of Solids* (Freeman, San Francisco, 1980), p. 253.

[20]W. A. Harrison and J. Tersoff, J. Vac. Sci. Technol. B **4**, 1068 (1986).

[21]J. Tersoff, Phys. Rev. B **30**, 4874 (1984).

[22]J. Tersoff, Phys. Rev. B **32**, 6968 (1985).

[23]I. P. Batra, Phys. Rev. B **29**, 7108 (1984).

[24]L. Kleinman, Phys. Rev. **128**, 2614 (1962).

[25]L. Kleinman, Phys. Rev. B **24**, 7412 (1981).

[26]W. E. Pickett, S. G. Louie, and M. L. Cohen, Phys. Rev. B **17**, 815 (1978); J. Ihm and M. L. Cohen, *ibid.* **20**, 729 (1979); W. E. Pickett and M. L. Cohen, *ibid.* **18**, 939 (1978).

[27]D. M. Ceperley and B. J. Alder, Phys. Rev. Lett. **45**, 566 (1980); J. Perdew and A. Zunger, Phys. Rev. B **23**, 5048 (1981).

[28]P. Bendt and A. Zunger, Phys. Rev. B **26**, 3114 (1982).

[29]A. Baldereschi, Phys. Rev. B **7**, 5212 (1973); D. J. Chadi and M. L. Cohen, *ibid.* **8**, 5747 (1973); H. J. Monkhorst and J. D. Pack, *ibid.* **13**, 5188 (1976); A. H. MacDonald, *ibid.* **18**, 5897 (1978).

[30]An increase in cutoff from 12 to 18 Ry affects the conduction-band energy of the Γ state significantly, and has a small effect upon *L*. Other energies are essentially converged with the 12-Ry cutoff.

[31]G. B. Bachelet and N. E. Christensen, Phys. Rev. B **31**, 879 (1985).

[32]In cases where the "unrepresentative" bands, such as the conduction band at Γ, would constitute the lowest energy gap, they should be placed relative to the representative ones.

[33]G. A. Baraff and M. Schlüter, in *Defects and Radiation Effects in Semiconductors, 1980,* Inst. Phys. Conf. Ser. No. 59, edited by R. R. Hasiguti (IOP, London, 1981), p. 287.

[34]M. Cardona, G. Harbecke, O. Madelung, and U. Rössler, *Physics of Group IV Elements and III-V Compounds,* Vol. 17a of *Landolt-Börnstein: Numerical Data and Functional Relationships in Science and Technology,* edited by O. Madelung (Springer, New York, 1982), Group III.

[35]F. H. Pollak and M. Cardona, Phys. Rev. **172**, 816 (1968).

[36]N. E. Christensen, Solid State Commun. **50**, 177 (1984).

[37]L. D. Laude, F. H. Pollak, and M. Cardona, Phys. Rev. B **3**, 2623 (1971).

[38]M. Chandrasekhar and F. H. Pollak, Phys. Rev. B **15**, 2127 (1977).

[39]C. Herring and E. Vogt, Phys. Rev. **101**, 944 (1956).

[40]I. Balslev, Phys. Rev. **143**, 636 (1966).

[41]E. O. Kane, Phys. Rev. **178**, 1368 (1969).

[42]J. A. Vergés, D. Glötzel, M. Cardona, and O. K. Andersen, Phys. Status Solidi B **113**, 519 (1982).

[43]R. M. Martin and C. G. Van de Walle, Bull. Am. Phys. Soc. **30**, 226 (1985).

[44]G. Abstreiter, H. Brugger, T. Wolf, H. Jorke, and H. J. Herzog, Phys. Rev. Lett. **54**, 2441 (1985).

[45]D. V. Lang, R. People, J. C. Bean, and A. M. Sergent, Appl.

Phys. Lett. **47**, 1333 (1985).

[46]R. Braunstein, A. R. Moore, and F. Herman, Phys. Rev. **109**, 695 (1958). These values were derived at 296 K; we have shifted them upward by approximately 0.1 eV, which should bring them close to the $T=0$ K values.

[47]T. F. Kuech, M. Mäenpää, and S. S. Lau, Appl. Phys. Lett. **39**, 245 (1981).

[48]G. Margaritondo, A. D. Katnani, N. G. Stoffel, R. R. Daniels, and Te-Xiu Zhao, Solid State Commun. **43**, 163 (1982).

[49]P. H. Mahowald, R. S. List, W. E. Spicer, J. Woicik, and P. Pianetta, J. Vac. Sci. Technol. B **3**, 1252 (1985).

[50]R. People, J. C. Bean, D. V. Lang, A. M. Sergent, H. L. Störmer, K. W. Wecht, R. T. Lynch, and K. Baldwin, Appl. Phys. Lett. **45**, 1231 (1984); R. People, J. C. Bean, and D. V. Lang, J. Vac. Sci. Technol. A **3**, 846 (1985).